MODELING AND DYNAMIC SIMULATION OF VARIABLE SPEED PUMP STORAGE UNITS INCORPORATED INTO THE GERMAN ELECTRIC POWER SYSTEM

K. Grotenburg, F. Koch, I. Erlich
Department of Electrical Power Systems
University of Duisburg, Germany
ean@uni-duisburg.de

U. Bachmann
Vereinigte Energiewerke AG VEAG
Berlin, Germany
udbachmann@veag.de

Keywords

Adjustable Speed Generation Systems, Double Fed Machine, Multivariable Control, Pump Storage Power Plant, Power System Simulation

Abstract

This paper deals with the modeling of variable speed pump storage power plant units equipped with double fed induction machine drives. The model is intended for use in a multi-machine simulation environment. The intention is to investigate the dynamic interaction between large variable speed units and the interconnected power system. First, a reduced order model of the double fed machine is developed. Based on this, a systematic multivariable controller design with dead-beat controller approach and terminal voltage compensation is carried out. The model is completed by voltage, power and speed controllers. Simulation results show the dynamic behavior of the new Goldisthal variable speed units in the German electrical power system.

1 Introduction

The German electric power company VEAG is going to build the new pump storage power plant called Goldisthal with a total capacity of 1060 MW in the south area of Thuringia/Germany. Two units will be built as variable speed drives with double-fed induction machines (DFIM). The other two units are equipped with conventional synchronous machines. The DFIM units are able to vary the speed in the range of 300 to 347 r.p.m. The converter feeding the rotor circuits has a rated power of 50 MVA, which is approximately only 20% of the total unit power. With this technique, the efficiency can be improved and a part-load pump mode will be possible [1]. Furthermore, the units are intended to be used for power-frequency-control as well.

Because of the high power, it is expected that the units have a significant effect on the system dynamic behavior. To explore the impact of Goldisthal on the network, it was necessary to involve the variable speed units into the dynamic simulation carried out regularly by the VEAG. The power system which is commonly investigated, consist of several hundreds synchronous generators and asynchronous motor loads. The network comprises nearly the entire European interconnected power system. The interesting dynamic phenomenons have a frequency range of 0.1-10 Hz. The restriction on these frequencies allows to describe the network inclusive the stator circuits of induction machines by algebraic equations, whereas the rotor side and all controllers are modeled by differential equations.

The simulation of the whole system with DFIM requires a DFIM-model, which is matching the model accuracy and the level of model aggregation with other rotating machines included into the system. In the following chapter, we will show the main characteristics of modeling and simulation at first. Resulting from these, the model of DFIM will be developed, which allows the application of a systematic multivariable controller design. The controller presented in this paper features not only a decoupling of both control channels for active and reactive power, but also a compensation of terminal voltage changes. We will show a DFIM controller with finite step response time behavior.

This core controller structure, completed by other second level regulators has been used to simulate the time behavior of the Goldisthal variable speed units in interaction with the German power system. All computer simulations were carried out with the power system simulation package PSD (Power System Dynamics) [2].

2 Basics of Modeling and Simulation

Our investigations are focused on electromechanical oscillations, which are caused by the rotor movements of electrical machines. The low frequencies of 0.1-10 Hz allow the use of reduced order system models and thus the simulation of large electric power systems. The basic reduction results from the neglecting of the transformer terms in the stator voltage equations [3]. That means, that the stator circuits and consequently the whole network can be described by algebraic equations. Assuming linear parameters, the most efficient solution of these equations is done by the complex nodal point method. Non-linear equations, caused e.g. by non-linear loads, can be solved iteratively. Rotor electrical circuits and rotor mechanical motions are modeled by differential equations because these parts affect mainly the interesting time behavior. Rotor flux linkages form an internal subtransient driving voltage, which is converted into a driving current for the solution of network equations.
Common power plant units comprise a complex system of regulator equipments. Due to the complexity and diversity of the technical solutions, the modeling of these parts requires a more flexible technique. For this purpose in our simulation package a powerful block-oriented user-defined modeling technique is implemented. Together with real controllers, block-oriented models are used for boilers, turbines and the excitation system as well. The two output variables are the excitation voltage and the mechanical torque, which are feeding the fix synchronous machine model. Fig. 1 gives an overview about the model and simulation structure.

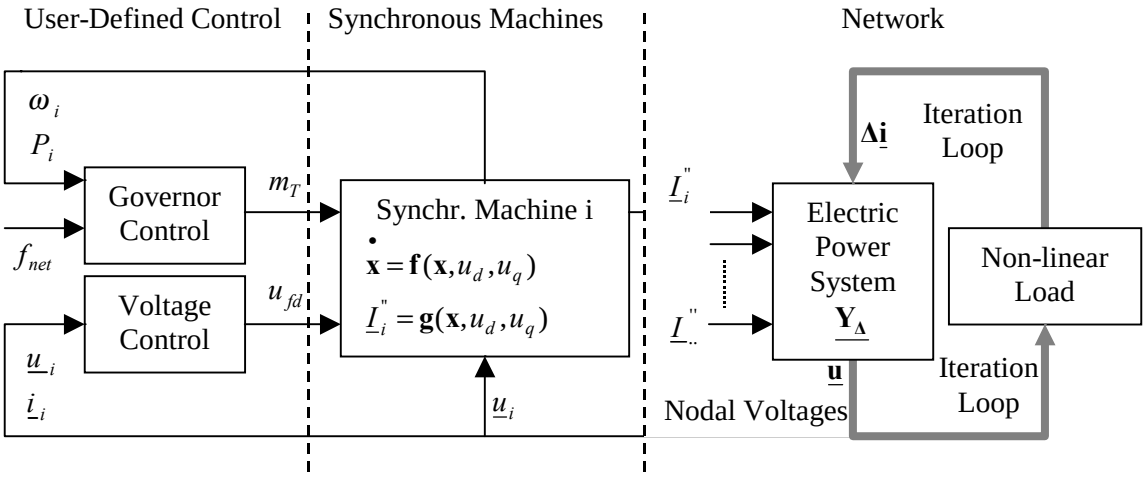

Fig. 1: Modeling and simulation structure

The common simulation time period reaches from one second to a few minutes. Taking into consideration, that several hundred machines are incorporated into the system, sophisticated numerical algorithms are necessary for solving the algebraic and differential equations.
DFIM models have to be included into the described simulation environment. Due to the desired frequencies, a reduced order model, similar to them of synchronous machines is adequate. In the next chapter this model of DFIM will be analytically developed.

3 Model of Double-Fed Induction Machines

The DFIM can be described as an asynchronous machine with the extension of a complex rotor voltage, which is the output of the cycloconverter [4]. Due to the symmetry of the machines complex space phasor equations for both, stator and rotor in an orthogonal rotating reference frame $\angle K$ is used. The machine is fully described by the equations (1)-(5), whereas per-unit quantities are assumed.

$$\underline{u}_S^{\angle K} = r_S \cdot \underline{i}_S^{\angle K} + \frac{d\underline{\psi}_S^{\angle K}}{dt} + j \cdot \omega_K \cdot \underline{\psi}_S^{\angle K} \tag{1}$$

$$\underline{u}_R^{\angle K} = r_R \cdot \underline{i}_R^{\angle K} + \frac{d\underline{\psi}_R^{\angle K}}{dt} + j \cdot (\omega_K - \omega_R) \cdot \underline{\psi}_R^{\angle K} \tag{2}$$

$$\underline{\psi}_S^{\angle K} = l_S \cdot \underline{i}_S^{\angle K} + l_h \cdot \underline{i}_R^{\angle K} \tag{3}$$

$$\underline{\psi}_R^{\angle K} = l_h \cdot \underline{i}_S^{\angle K} + l_R \cdot \underline{i}_R^{\angle K} \tag{4}$$

$$\frac{d\omega_R}{dt} = \frac{1}{T_m}\left(m_T + \psi_{Sd} i_{Sq} - \psi_{Sq} i_{Sd}\right) \tag{5}$$

Neglecting stator transients means that

$$\frac{d\underline{\psi}_S^{\angle \omega_0}}{dt} = 0 \tag{7}$$

will be set in the voltage equation (1), whereas this step is done in a synchronously rotating reference frame. The theoretical background of this model reduction is discussed in [2]. An alternative way is to set $\omega_K = \omega_0$ in Eq. (1) additionally to Eq. (7). The result is the following algebraic equation describing the stator circuits.

$$\underline{u}_S^{\angle K} = r_S \cdot \underline{i}_S^{\angle K} + j \cdot \omega_0 \cdot \underline{\psi}_S^{\angle K} \tag{8}$$

Substituting $\underline{\psi}_S^{\angle K}$ by

$$\underline{\psi}_S^{\angle K} = l_S \cdot \underline{i}_S^{\angle K} + \frac{l_h}{l_R}\left(\underline{\psi}_R^{\angle K} - l_h \underline{i}_S^{\angle K}\right) \tag{9}$$

which follows from Eq. (3) and (4) the transient inductance resp. coupling factor, defined by the equations (10) and (11)

$$l' = l_h + l_{\sigma S} - \frac{l_h^2}{l_h + l_{\sigma R}} \tag{10}$$

$$k_R = \frac{l_h}{l_h + l_{\sigma R}} \tag{11}$$

we get

$$\underline{u}_S^{\angle K} = (r_S + j\omega_0 l') \cdot \underline{i}_S^{\angle K} + j\omega_0 k_R \underline{\psi}_R^{\angle K} \tag{12}$$

The transient driving voltage of the machine is now

$$\underline{u}' = j\omega_0 k_R \underline{\psi}_R^{\angle K} \tag{13}$$

behind of the transient reactance

$$\underline{z}' = (r_S + j\omega_0 l') \tag{14}$$

The equivalent driving current to $\underline{u}_S^{'}$ is

$$\underline{i}^{'} = -\frac{\underline{u}^{'}}{\underline{z}^{'}} \tag{15}$$

which is coupling the machine with the algebraic network equations. The rotor voltage equation (2) gets the following form after rotor and stator current respectively stator flux linkage are eliminated using Eq. (4), (8) and (12).

$$\frac{d\underline{\psi}_R^{\angle K}}{dt} = -(\underline{T}_{L0}^{-1} + \frac{j \cdot \omega_0 \cdot k_R^2 \cdot r_R}{\underline{z}^{'}}) \cdot \underline{\psi}_R^{\angle K} + \frac{r_R \cdot k_R}{\underline{z}^{'}} \cdot \underline{u}_S^{\angle K} + \underline{u}_R^{\angle K} \tag{16}$$

$$\underline{T}_{L0}^{-1} = \frac{r_R}{l_R} + j \cdot (\omega_K - \omega_R) \tag{17}$$

The orientation is now to a state space form with the state variables rotor flux linkages $\underline{\psi}_R^{\angle K}$ and the terminal voltages from the stator and rotor side $\underline{u}_S^{\angle K}$ and $\underline{u}_R^{\angle K}$ as input variables.

The components of the rotor voltage can be controlled via cycloconverter, whereas the complex stator terminal voltage is interpreted as a disturbance variable mainly influenced by the behavior of the network. From Eq. (12) follows for the stator current

$$\underline{i}_S^{\angle K} = \frac{\underline{u}_S^{\angle K} - j\omega_0 k_R \underline{\psi}_R^{\angle K}}{(r_S + j\omega_0 l')} \tag{18}$$

Actually, stator current is used as control variable instead of the rotor flux linkage $\underline{\psi}_R^{\angle K}$, which is badly measurable. However, for better understanding, the derivation of controller in the following chapter will be carried out with $\underline{\psi}_R^{\angle K}$. From the point of view of the control theory, the electrical part of process is fully described by the Eq. (12), (16) resp. (18). The system has a bilinear character because of the product of $\underline{\psi}_R^{\angle K}$ and ω_K [5] in the state equation (16). But, ω_K can be chosen so, that it remains approximately constant in each integration step, e.g. by setting $\omega_K = \omega_{Net}$, because the network frequency ω_{Net} is a slow variable. For the simulation, we need also the differential equation of motion, which get now from Eq. (5) the following form

$$\frac{d\omega_R}{dt} = \frac{1}{T_m}\left(m_T + \psi_{Rd} i_{Sq} - \psi_{Rq} i_{Sd}\right) \tag{19}$$

4 Design of a Multivariable Controller

In a first step, the state equation (16) will be transformed into the time-discrete vector equation (20)

$$\mathbf{\Psi}_R^{\angle K}(k+1) = \mathbf{\Phi}(\omega_R, \omega_K) \cdot \mathbf{\Psi}_R^{\angle K}(k) + \mathbf{H} \cdot \mathbf{u}_R^{\angle K}(k) + \mathbf{h} \cdot \mathbf{u}_S^{\angle K}(k) \tag{20}$$

The following control approach

$$\mathbf{u}_R^{\angle K}(k) = \mathbf{H}^{-1} \cdot \left[\mathbf{y}^{\angle K}(k-1) - \mathbf{h} \cdot \mathbf{u}_S^{\angle K}(k)\right] \tag{21}$$

where $\mathbf{y}^{\angle K}$ is the output of the regulator, allows a compensation of the disturbance variables $\mathbf{u}_S^{\angle K}(k)$ [6]. It can be seen by substituting $\mathbf{u}_R^{\angle K}(k)$ in Eq. (20)

$$\mathbf{\Psi}_R^{\angle K}(k+1) = \mathbf{\Phi}(\omega_R, \omega_K) \cdot \mathbf{\Psi}_R^{\angle K}(k) + \cdot \mathbf{y}^{\angle K}(k-1) \tag{22}$$

and z-transformed:

$$(z\mathbf{I}-\mathbf{\Phi})\cdot\mathbf{\Psi}_R^{\angle K}(z)=z^{-1}\cdot\mathbf{y}^{\angle K}(z) \tag{23}$$

The approach for the control equation is now

$$\mathbf{y}^{\angle K}(z)=\mathbf{R}\cdot(\mathbf{\Psi}_R^{\angle K^*}(z)-\mathbf{\Psi}_R^{\angle K}(z)) \tag{24}$$

where $\mathbf{R}$ is the controller matrix and $\mathbf{\Psi}_R^{\angle K^*}(z)$ the reference value of the controlled variable. The structure of $\mathbf{R}$ depends on the target function, which has to be met. For a dead-beat behavior, defined by the following equation

$$\mathbf{\Psi}_R^{\angle K}(z)=z^{-2}\cdot\mathbf{\Psi}_R^{\angle K^*}(z) \tag{25}$$

we get

$$\mathbf{R}_{DB}=\frac{1}{1-z^{-2}}\cdot(\mathbf{I}-z^{-1}\cdot\mathbf{\Phi}) \tag{26}$$

Dead-beat controllers belonging to the controllers with finite step response time behavior, which are characterized by the feature, fully adjusting the control deviation in n+1 steps. For two and three steps yields:

n = 2: $\mathbf{\Psi}_R^{\angle K}(z)=\frac{1}{2}\cdot(z^{-2}+z^{-3})\cdot\mathbf{\Psi}_R^{\angle K^*}(z)$ ➔ $\mathbf{R}_{n-2}=\frac{1+z^{-1}}{2-z^{-2}-z^{-3}}\cdot\left(\mathbf{I}-z^{-1}\cdot\mathbf{\Phi}\right)$

n = 3: $\mathbf{\Psi}_R^{\angle K}(z)=\frac{1}{3}\cdot(z^{-2}+z^{-3}+z^{-4})\cdot\mathbf{\Psi}_R^{\angle K^*}(z)$ ➔ $\mathbf{R}_{n-3}=\frac{1+z^{-1}+z^{-2}}{3-z^{-2}-z^{-3}-z^{-4}}\cdot\left(\mathbf{I}-z^{-1}\cdot\mathbf{\Phi}\right)$

The controllers are in the last both cases more complex, but the required control energy is less. Therefore, such controllers are more favorable in technical realizations. The controller structure is shown in Fig. 2.

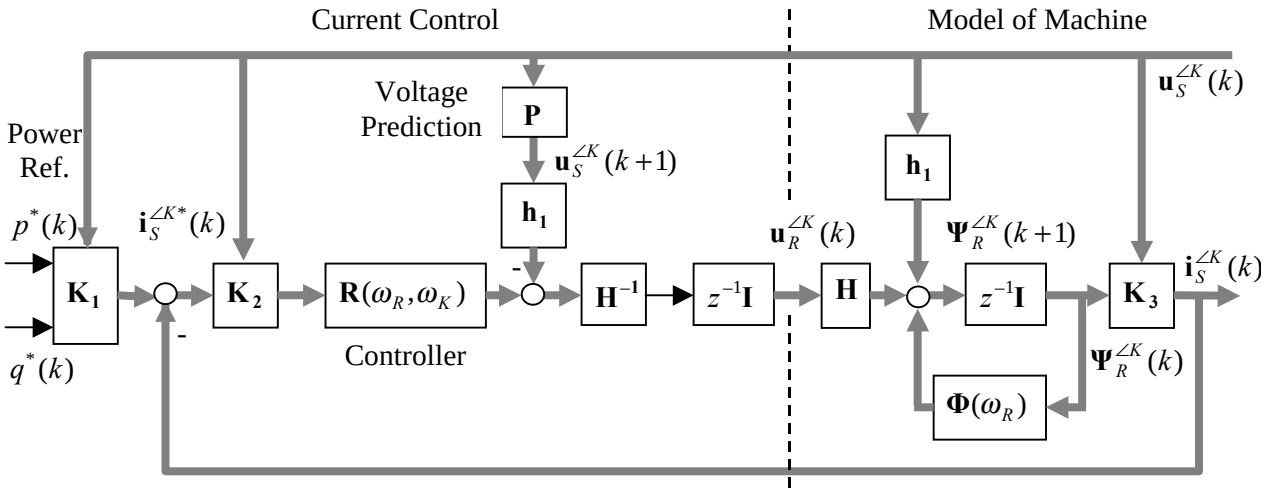

Fig. 2: DFIM controller

Because the rotor flux linkages are not measurable directly, the controller is extended by two blocks $\mathbf{K_2}$ and $\mathbf{K_3}$, which are included for conversion between $\mathbf{\Psi}_R^{\angle K}(k)$ and $\mathbf{i}_S^{\angle K}$ based on Eq. (12) and (18) respectively. The reference signal $\mathbf{i}_S^{\angle K^*}(k)$ is derived from the corresponding values of active and reactive power. One of the main features of this controller is its ability to compensate stator terminal voltage changes. However, for this purpose we need $\mathbf{u}_S^{\angle K}(k+1)$, which is unknown and therefore must be predicted. We made good experience with a linear extrapolation described by the transfer function $\mathbf{P}=2-z^{-1}$. The controller is fully modeled by the block-oriented technique, which allows

the required flexibility. The DFIM model is integrated into the fix programmed part and thus very fast.
As an example, Fig.3 shows the time response of the system working on an infinite bus, to a step change of the reactive power reference value $\Delta q^*(k)$. As can be seen, the controller needs four steps according to the applied controller matrix for raising the reactive power, whereas the active power remains nearly constant. That means that the control channels are decoupled. The results are similar by computing a step response in the active power channel.
The controller equations contain also ω_k as parameter, which is the speed of the reference frame and still must be chosen properly. Setting $\omega_k = \omega_{Net}$, as mentioned in the previous chapter, in cases of a permanent network frequency drop, all controller variables will remain in steady state. Furthermore, the controller will work more accurate. With any other ω_k, the variables of the controller would change continuously.

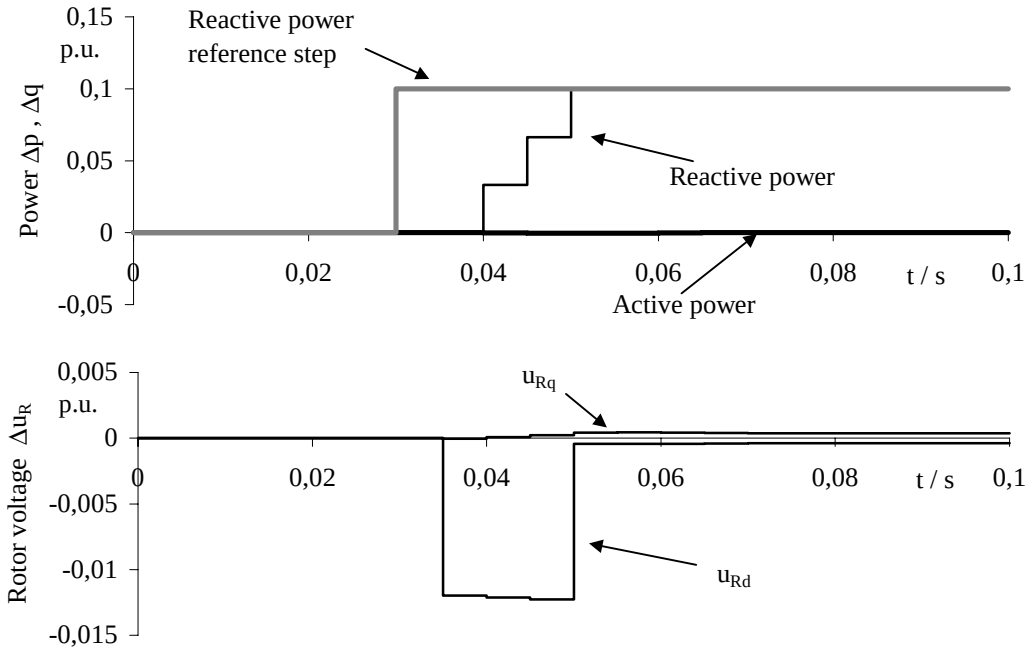

Fig. 3: Step response of the system Controller-DFIM-Infinite-Bus to a reactive power step

5 Modeling of the pump storage power plant unit

For the simulation of the behavior of a pump storage power plant unit, it is necessary to complete the model by second level controllers. The structure and functionality differ slightly in generator and pump modes [7]. Fig. 4 gives an overview about the model we have implemented for generator mode.

The voltage and active power controllers are working to the inputs of the stator current controller directly. The reference value of the active power controller can be modified by the speed and network frequency controllers as well. The first one is activated only when an unreasonable speed deviation occurred. It makes sure, that the speed will be controlled back into the required speed range. With the network frequency control, the unit is able to participate in the primary control of the power system. In contrary to classical synchronous machine units, the control deviation is conducted, beside to the turbine, also to the active power controller, which is operating on the electrical rotor circuits. This regulator channel is much more faster then the turbine.

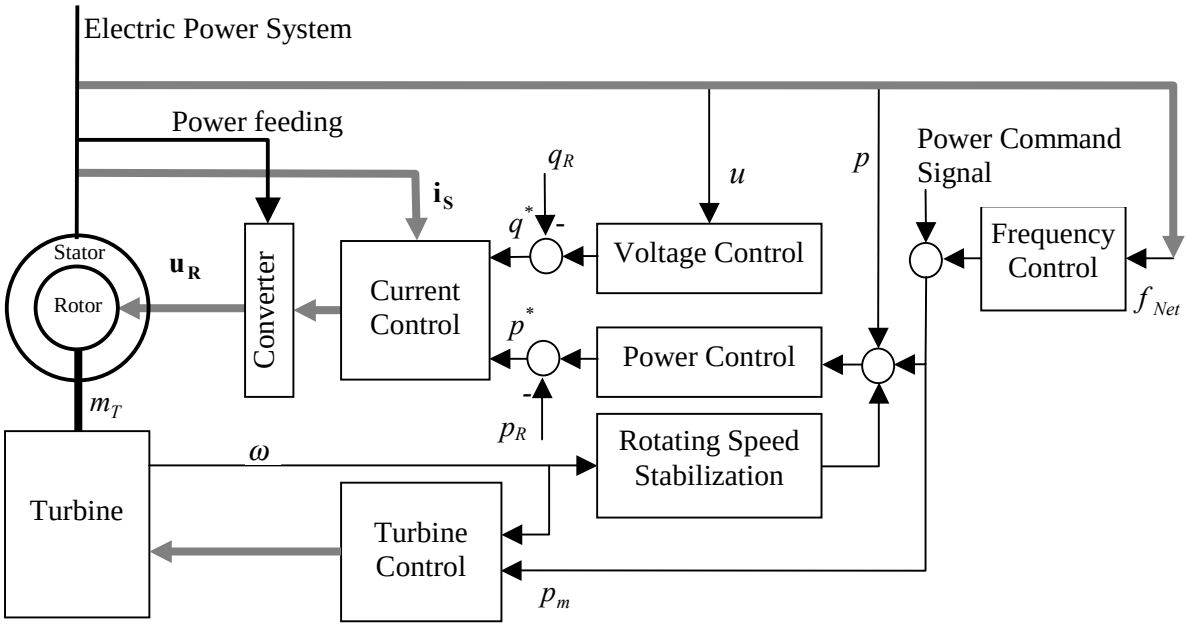

Fig. 4: Model for generator mode

However, the ancillary energy supplied to network is charged by the kinetic energy of the rotor, which will be, in the consequence decelerated. Therefore, it is necessary to replace the energy supply by the turbine after a short period. Nevertheless, the DFIM unit provides an excellent mean for a fast power control. In our application the active power on the network side, which is the sum DFIM and converter powers, is controlled. Because the current control is developed for the stator terminal quantities, the output of the power controller must be adjusted to the machine by subtraction of the current rotor power.
The turbine model we have used bases on the references [8], [3]. This controller and the associated hydraulic equipments are also on classical hydro turbines existent and therefore, this topic will not be discussed here more closely.
The total power of the unit is consisting of the stator and rotor powers. In our simulation, no losses are assumed for converter. Calculating the prefault steady state, the unit power delivered by a standard load flow program, must be splitted into these both parts. It can be carried out iteratively. We have implemented for this purpose a simplified Newton algorithm. The speed of the unit is set as an optimum for the given operating point. To get the speed depending on the actual power, the water head and the operating mode a characteristic function describing the specific unit is used in the simulation.

6 Simulation result with the Goldisthal units

The new pump storage power plant of the German electric power company VEAG is located in Thuringia. The first unit will go in operation in 2002/2003. Two of the four units will build with variable speed DFIM because of the better efficiency and flexibility in part load mode. The machines will have a rated power of 265 MW and a synchronous speed of 333 r.p.m., whereas the speed will varied between +4/-10%. It requires a converter power of approximately 50 MVA. The mean water head is 302 m. The upper water basin has a storage capacity of $12*10^6$ m^2 water. Goldisthal is connected to the VEAG high voltage network via a 380 kV double circuit tie line.
The investigations to the dynamic behavior of the new variable speed units were carried out in the preliminary project stages, so that no proper specifications were available to the control concept and machine parameter. On the other hand, the interest was focused on the dynamic interaction between the variable speed units and the network. For this purpose, a model of DFIM and regulators described

above was used. The electrical power system of the VEAG was modeled in detail together with other parts of the UCTE system. The full system consists of several hundreds synchronous generators and thousands of lines and nodes.
The following two simulation examples should demonstrate the dynamic capabilities of the units with DFIM drive in comparison with traditional synchronous machines. Fig. 5 shows results where a three-phase short circuit in a distance network location was simulated. In the consequence of the short circuit, the terminal voltage in Goldisthal breaks down to 0.7 p.u. approximately. During the short circuit period, synchronous machines cannot supply the full power into the network (see Fig. 5a). The difference between electrical and mechanical torque accelerates the rotor, which could be dangerous regarding transient stability. Despite of the very low voltages, variable speed units are able raising the active power back to the steady state value even in the short circuit period (see Fig. 5b). After then, a normal operating point will reached much faster then in the case of synchronous machines.

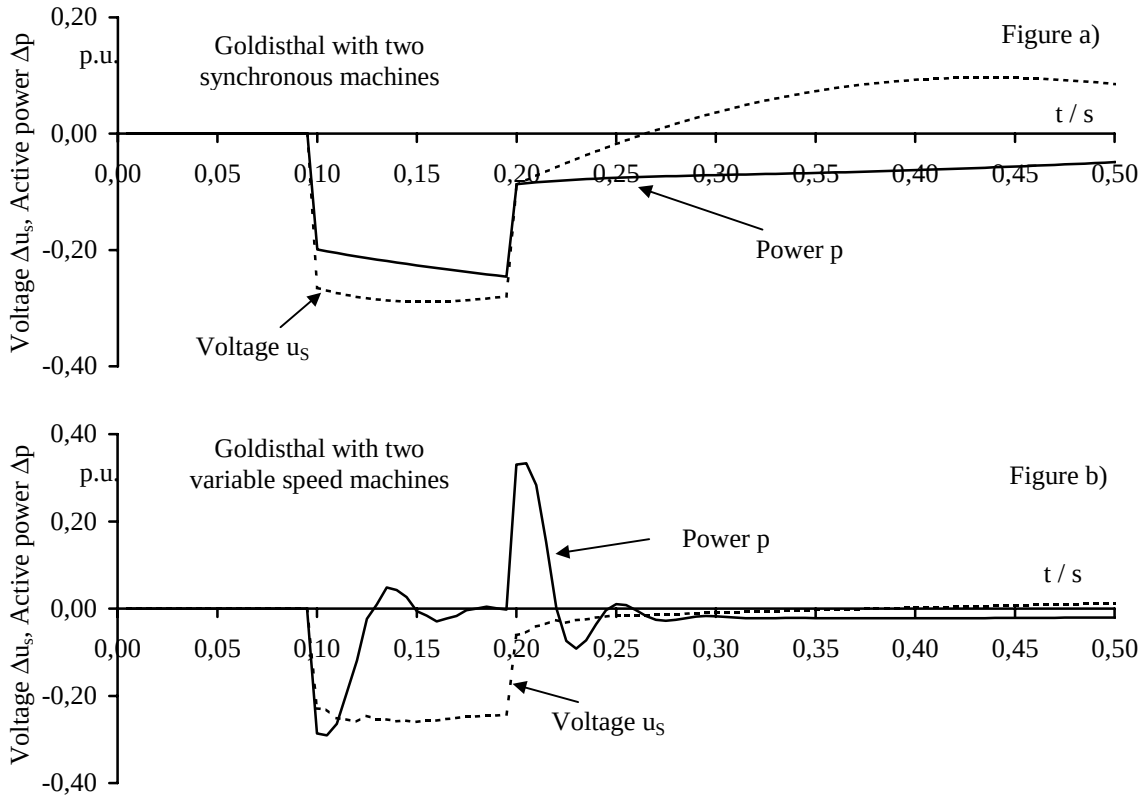

Fig. 5: Time behavior of the Goldisthal variable speed units by a network distance short circuit

The second example in Fig. 6 shows the time response of the variable speed units to an active power reference step of 2 %.
The required power on the grid side will be reached after approx. 2 sec fully charged by rotor kinetic energy. Because the water flow through the hydro turbine does not change immediately when the gate is suddenly opened, the initial surge of the turbine is opposite. Therefore, the electrical power regulator has even to activate more power then the required reference step. After 10 sec the turbine is now able to cover the energy. Then, the turbine speed control makes sure that the rotor speed will return to the steady states value corresponding with the current power reference. Synchronous machine units change the electrical power only according to turbine power changes. Therefore, the time response in this case would take much longer.

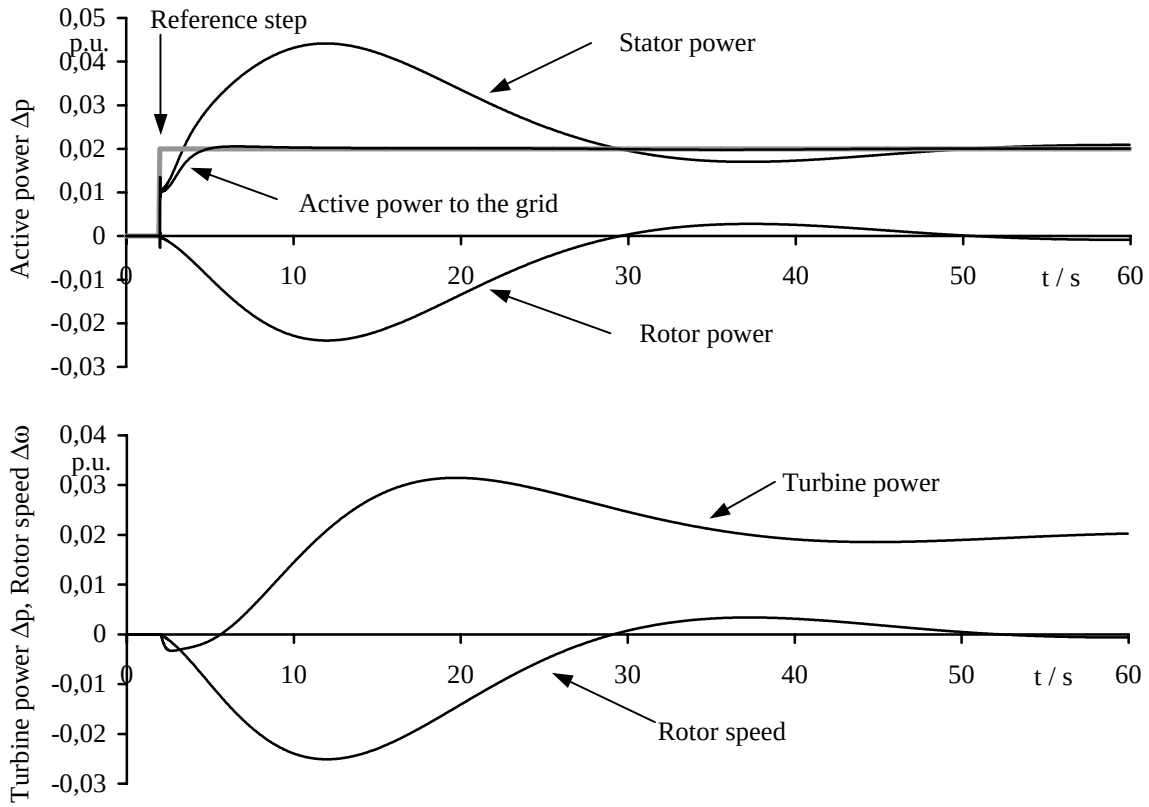

Fig. 6 : Time response of the variable speed unit to an active power reference step of 2%

7 Conclusions

Large pump storage power plants with variable speed drives have a considerable effect on the dynamic behavior of electric power systems. DFIM meets the requirements for such drives. On one side, the speed can be varied in a range, which is sufficient for this purpose. On the other hand, the converter rated power remains constrained.

In this paper, a reduced order model for the simulation of multi-machine electric power systems comprising DFIM drives has been developed. The model describes the DFIM on the same aggregation level as synchronous machine models established in the simulation practice. Thus, the calculation of large electrical power systems with variable speed pump storage drives becomes possible, without the assumption of a constant terminal voltage. The systematic design of a multivariable controller applied to the DFIM, leads to a stator current controller with two channels, which are dynamically and stationary decoupled. Furthermore, the controller approach we have applied allows the compensation of stator terminal voltage changes by predicting the voltage for the next step. The model completed by voltage, power, speed and network frequency as well as turbine controllers has been used to simulate the dynamic behavior of the Goldisthal variable speed pump storage units in the interconnected German power system. The simulation results show an excellent dynamic behavior of the Goldisthal units.

References

[1] Bogenrieder W.; Lein G.: Leistungsfrequenzregelung mit Pumpturbinensätzen variabler Drehzahl am Beispiel des Pumspeicherwerkes Goldisthal (Load-Frequency-Control of Pump Storage Power Units in case of Goldisthal), VDI-Reports 1529, 2000, pp. 241 - 255.
[2] Erlich, I.: Analyse und Simulation des dynamischen Verhaltens von Elektroenergiesystemen (Analysis and Simulation of the Dynamic Behavior of Electrical Power Systems), Habilitation-Thesis, Technical University of Dresden, Department of Electrical Engineering, 1995.
[3] Kundur, P.: Power System Stability and Control, McGraw-Hill, 1994.
[4] Dittrich A.; Hofmann W.; Stoev A.; Thierme A.: Design and Control of a Wind Power Station with Double-fed Induction Generators, EPE Trondheim, 1997, pp. 2.723 – 2.728.
[5] Schwarz H.: Nichtlineare Regelungssysteme (Non linear Control Systems), Oldenbourg Verlag, 1991.
[6] Quang N.P.; Dittrich J.-A.: Praxis der feldorientierten Drehstromantriebsystemregelung (Paxis of the field-oriented Drives Control) Book, Expert Verlag, 1999.
[7] Kuwabara T.; Harada M.; Bando A.: Performance of 400 MW Adjustable Speed Pumped Storage Unit for Ohkwachi Power Station, NE-Vol. 15, ASME, 1994, pp. 1 - 10.
[8] IEEE Working Group: Dynamic Models for Steam and Hydro Turbines in Power System Studies, IEEE Committee report, PES Winter Meeting New York, 1973, pp. 1904 - 1915.

Nomenclature

f_{Net}	actual frequency of power system
$\mathbf{H}$	time-discrete control-matrix
$\mathbf{h}$	time-discrete disturbance-matrix
$\mathbf{I}$	unit matrix
$\underline{I}''$	driving current
$\underline{i}_R$	complex rotor-current
$\underline{i}_S$	complex stator-current
k	sampling step
k_R	coupling-factor
l_S	stator-inductance
l_R	rotor-inductance
l_h	main-inductance
l_σ	leakage-inductance
m_T	torque of turbine-shaft
n	total number of steps
r_S	stator-resistance
r_R	rotor-resistance
$\mathbf{R}$	control transfer function (matrix)
$\mathbf{R}_{DB}$	control matrix, Dead-Beat-controller
$\mathbf{R}_{n-2}$	control matrix, finite step response time
$\mathbf{R}_{n-3}$	control matrix, finite step response time
T_m	inertia constant
u_{fd}	excitation voltage
$\underline{u}_S$	complex stator-voltage
$\underline{u}_R$	complex rotor-voltage
$\mathbf{u}_S$	vector of stator-voltage
$\mathbf{u}_R$	vector of rotor-voltage
$\mathbf{x}$	state vector
$\mathbf{y}$	output-matrix of regulator
$\underline{\mathbf{Y}}_N$	nodal admittance matrix
z	z-operator
$\underline{z}$	complex impedance
$\mathbf{\Phi}$	discrete transition matrix
$\underline{\psi}_R$	complex rotor-flux-linkage
$\underline{\psi}_S$	complex stator-flux- linkage
$\mathbf{\Psi}_R$	vector of rotor-flux- linkage
$\mathbf{\Psi}_S$	vector of stator-flux- linkage
ω_0	synchronous angular velocity
ω_K	angular velocity of the reference frame
ω_R	angular velocity of rotor
ω_{Net}	power system network angular velocity

Up set index

$\angle K$	labeling variables in with ω_K-rotating reference frame
$\angle\omega_0$	synchronous rotating reference frame
*	labeling of reference values
′	transient variable
″	subtransient variable

Down set index

d	d-axis of rotating reference frame
q	q-axis of rotating reference frame
R	rotor variable
S	stator variable
T	turbine